Analytica Chimica Acta 683 (2011) 242–247

Contents lists available at ScienceDirect

Analytica Chimica Acta

journal homepage: www.elsevier.com/locate/aca

High-sensitivity biosensors fabricated by tailoring the localized surface plasmon resonance property of core–shell gold nanorods

Haowen Huang[a,*], Shaowen Huang[a], Shishan Yuan[b], Caiting Qu[a], Yi Chen[c,**], Zhongjian Xu[a], Bo Liao[a], Yunlong Zeng[a], Paul K. Chu[d]

[a] Key Laboratory of Theoretical Chemistry and Molecular Simulation of Ministry of Education, School of Chemistry and Chemical Engineering, Hunan University of Science and Technology, Xiangtan 411201, China
[b] Medical College of Hunan Normal University, Changsha, 410013, China
[c] Key Laboratory of Analytical Chemistry for Living Biosystems, Institute of Chemistry, Chinese Academy of Science, Beijing 100190, China
[d] Department of Physics & Materials Science, City University of Hong Kong, Tat Chee Avenue, Kowloon, Hong Kong, China

ARTICLE INFO

Article history:
Received 22 August 2010
Received in revised form 18 October 2010
Accepted 22 October 2010
Available online 31 October 2010

Keywords:
Localized surface plasmon resonance
Gold nanorod composite
Schistosomiasis japonica
Biosensor

ABSTRACT

An enhanced sensitive biosensor has been developed to detect biological targets by tailoring the localized surface plasmon resonance property of core–shell gold nanorods. In this new concept, a shell layer is produced on gold nanorods by generating a layer of chalcogenide on the gold nanorod surface after attachment of the recognition reagent, namely, goat IgG and antigen of schistosomiasis japonica. The bioactivity of these attached biomolecules is retained and the sensitivity of this biosensor is thus enhanced significantly. The plasmonic properties of the gold nanorods attached with the biomolecules can be adjusted and the plasmon resonance wavelength can be red-shifted up to several hundred nanometers in the visible or near infrared (NIR) region, which is extremely important to biosensing applications. This leads to a lager red-shift in the localized surface plasmon resonance absorption compared to the original gold nanorod-based sensor and hence offers greatly enhanced sensitivity in the detection of schistosomiasis japonica. The human serum infected with schistosomiasis japonica diluted to 1:50,000 (volume ratio, serum/buffer solution) can be detected readily. The technique offers enhanced sensitivity and can be easily extended to other sensing applications based on not only immuno-recognition but also other types of specific reactions.

1. Introduction

Gold nanorods possess an anisotropic configuration and unique optical properties exhibiting transverse and longitudinal plasmon bands. The longitudinal plasmon band is extremely sensitive to changes in the dielectric properties in the surroundings, leading to strong, characteristic absorption bands in the visible to infrared part of the spectrum [1,2]. A significant change in the plasmon spectra in response to the change in the refractive index in the vicinity of the gold nanorods arises from the localized surface plasmon resonance (LSPR) properties and can be effectively utilized to detect specific target binding events. Recently, LSPR has been applied to the detection of DNA and other biomolecules using an analyte-induced aggregation/assembly of gold nanospheres [3–8]. Although the methodology is simple and relatively straightforward, the use of gold nanorods to detect biomolecules has obvious advantages compared to the use of gold nanospheres. The analyte-induced aggregation of spherical gold nanoparticle results in a decrease in the plasmon absorption at around 520 nm and formation of a long wavelength band. It introduces significant widening in the plasmon peak thereby reducing the spectral resolution which compromises specific detection [9–12]. In contrast, anisotropic gold nanorods offer both lateral and axial (end-to-end) configurations which give rise to unique transverse and longitudinal plasmon resonance absorption [13–16]. The longitudinal plasmon response to changes in the dielectric properties or refractive indices in the vicinity manifests in characteristic resonance absorption bands in visible to IR range [17]. This makes gold nanorods more attractive in simple, rapid, and selective sensing in bioanalytical chemistry [18–20].

Recent experiments have focused on gold nanorod composites in order to broaden the applications of gold nanorods [21–25]. Complex nanostructures containing these nanoparticles are more versatile from the perspective of applications if nanoparticles that combine multiple functions or properties not attainable by a single type of material can be developed. Hence, new nanoparticles that combine an optical signature with other physical properties are

* Corresponding author. Tel.: +86 731 58290045; fax: +86 731 58290509.
** Corresponding author.
E-mail addresses: hhwn09@163.com (H. Huang), chenyi@iccas.ac.cn (Y. Chen).

0003-2670/$ – see front matter © 2010 Elsevier B.V. All rights reserved.
doi:10.1016/j.aca.2010.10.033

particularly useful because they enable optical tracking or monitoring of specific species and particles. A useful strategy to monitor optical properties on the nanoscale involves integration of noble metals and associated localized surface plasmon into the particles or structures. As a result, complex nanoparticles, particularly core–shell nanostructures, are attractive in nanobiotechnology such as the analysis of biomolecules and other target species [26–28]. The capability of detecting biological molecules *in vitro* or *in vivo* with high sensitivity and selectivity in a small sample size is potentially achievable because of the distinctive electronic, optical, and magnetic properties of nanostructures.

In this paper, we report a novel method based on gold nanorod composites to measure the ligand-receptor binding with tailoring plasmonic properties. The plasmonic properties of the resulting nanocomposite can be adjusted. That is, the longitudinal plasmon wavelength (LPW) can be tailored to red-shift by up to several hundred nanometers in the visible or near infrared (NIR) range thereby boding well for biosensing applications. Moreover, a sensitive biosensor for schistosomiasis japonica fabricated by a shell technique on gold nanorods attached to antigen of schistosomiasis japonica is developed. Schistosomiasis is second to malaria among parasitic diseases and affects millions of people in developing countries in the tropical and subtropical parts of Africa, Asia and South America [29–31]. Therefore, it is very important to develop a simple and straightforward technique to detecting schistosomiasis japonica with high sensitivity. Compared to the indirect hemagglutination test (IHA) [32] for the diagnosis of schistosomiasis which tends to be labor intensive and not sensitive enough during early or light infection, the novel approach reported here is simpler and more sensitive.

2. Experimental

2.1. Materials

$HAuCl_4{\cdot}3H_2O$, cetyltrimethylammonium bromide (CTAB), $Na_2S_2O_3$, ascorbic acid, tris(hydroxymethyl) aminomethane and silver nitrate were purchased from Sinopharm Chemical Reagent Co., Ltd. (Shanghai, China). The goat IgG and rabbit anti goat IgG were obtained form Biodee Biotechnology Co., Ltd. (Beijing, China). N-hydroxysuccinimide (NHS) was purchased from ACROS (New Jersey, USA), N-ethyl-N-[(dimethylamino) propyl]carbodiimide (EDC) from Avocado Research Chemicals Ltd. (Lancashire, UK), and mercaptoundecanoic acid (MUA) from Aldrich (Milwaukee, USA). All the chemicals, unless mentioned otherwise, were all of analytical reagent grade and used as received. Aqueous solutions were prepared in doubly distilled water.

2.2. Instrumentation

Transmission electron microscopy (TEM) was performed on a JEM-2010 transmission electron microscope at 80 kV. Fourier transform infrared (FTIR) spectra were acquired from the functionalized gold nanorods mixed with dried KBr on the Spectrum one instrument manufacture by Perkin Elmer. The LSPR optical results were obtained from the nanorods on a UV–visible spectrophotometer (Lambda 35, Perkin Elmer).

2.3. Preparation of gold nanorods

The seed solution of gold nanorods was prepared according to the previously reported method [33,34]. CTAB solution (1.5 mL, 0.1 M) was mixed with 100 μL of 0.02 M $HAuCl_4$. 100 μL of ice cold 0.01 M $NaBH_4$ was added to the stirred solution resulting in the formation of a brownish yellow solution. Vigorous stirring was continued for 2 min and then the seed solution was kept at room temperature (25 °C) and used at least 2 h after preparation.

To synthesize the gold nanorods, 1.5 mL of 0.02 M $HAuCl_4$ and 1.0 mL of 0.01 M $AgNO_3$ were added to 30 mL of 0.1 M CTAB, followed by addition of 0.8 mL of 0.08 M ascorbic acid. Ascorbic acid worked as a mild reducing agent and changed the solution from dark yellow to colorless. Finally, 70 μL of the seed solution was added and the color of the solution gradually changed within 15 min.

2.4. Functionalization of gold nanorods

Functionalization of the gold nanorods took advantage of the well-known affinity between gold and thiol compounds. The gold nanorods were easily modified by alkanethiols to form SAMs to facilitate attachment to recognition agents (antibodies in this work). Chemical modification of gold nanorods was achieved according to the following: 0.5 mL of 20 mM ethanol solution of MUA was added to 5 mL of the gold nanorods suspension and it remained for at least 18 h under room temperature. Nanorods were then collected by centrifugation at 14,000 rpm for 12 min and resuspended in a 0.005 M CTAB solution. Afterwards, the activated nanorods were added to the freshly prepared EDC and NHS solution and sonicated for 30 min. The resulting nanorods were collected by centrifugation at 14,000 rpm for 12 min and then incubated in the goat IgG solution (0.01 g L^{-1}) containing 0.005 M CTAB. After the attachment of goat IgG onto the GNRs, the modified GNRs were collected by centrifugation at 14,000 rpm for 12 min and divided into two parts; one resuspended in a 10 mM Tris–HCl buffer solution (pH 7.4) containing 0.005 M CTAB and the other in 0.1 M CTAB solution.

2.5. Tailor plasmonic properties of fuctionalizational gold nanorods

50 μL of the 0.1 M $Na_2S_2O_3$ solution was added to 3 mL of the modified gold nanorods suspended in the 0.1 M CTAB solution. Extinction spectra were obtained from the nanorods on a spectrophotometer. Because the longitudinal plasmon wavelength (LPW) red-shifted with increasing reaction time, various stages were monitored from the tunable plasmonic band gold nanorods based on different reaction time intervals. The mixture of gold nanorods and $Na_2S_2O_3$ solution was taken out, centrifuged, and re-dispersed in water.

2.6. Expression and purification of rSjGST-32

The DNA sequence encoding schistosomiasis japonica 32 kDa protein was ligated into pGEX-5X-3, which encoded glutathione S-transferase (GST). Recombinant fusion protein rSjGST-32 was expressed in JM109 strain of *Escherichia coli* containing recombinant plasmid pGEX-5X-3–Sj32 when induced with 0.1 mM IPTG at 37 °C for 2 h. The cells were harvested by centrifugation, resuspended in a phosphate buffered saline (PBS) containing 0.1% Triton-X100, and sonicated (400 W) using an ultrasonic cell disruption apparatus. The cell debris was removed by centrifugation at 10,000 rpm for 20 min at 4 °C. rSjGST-32 was purified from the supernatant of bacterial lysate by glutathione affinity chromatography with a 1 mL GSTrap column (GE Healthcare) according to the operation guide and was analyzed by 12% SDS-PAGE under reduction conditions. The protein concentration was determined by Bradford assay using BSA as the standard.

2.7. Serum samples

The serum samples were supplied by Hunan Institute of Parasite Disease. 10 human serum samples infected with schistosomiasis

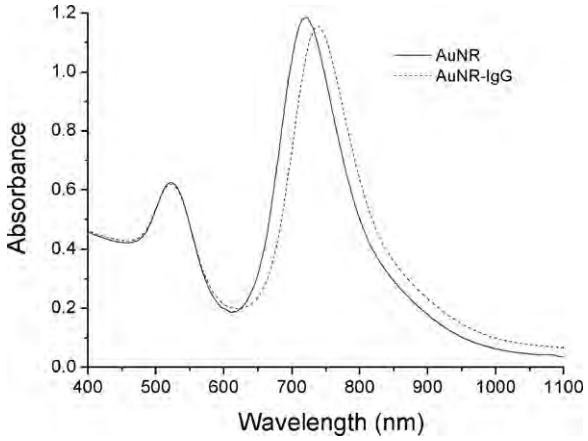

Fig. 1. Absorption spectra of gold nanorods before (solid line) and after (dash line) attachment of goat IgG.

japonica were collected. The eggs of schistosomiasis japonica were detected in their feces and antibodies to schistosomiasis japonica antigen in their sera tested by IHA. These serum samples were mixed as a test sample to investigate the optimal experimental conditions and 10 human serum samples were examined under the same conditions. Similarly, 10 normal human serum samples were collected for control experiments. Every sample was tested three times in parallel in this study.

3. Results and discussion

3.1. Tailoring localized surface plasmon property of functionalized gold nanorods

The innovation in this new approach lies in that the localized surface plasmon resonance property may be adjusted after attachment of the recognition reagent, namely the antigen of schistosomiasis, resulting in an enhancement of detection sensitivity. It should be noted that the bioactivity of the attached antigen of schistosomiasis japonica is still retained. The goat IgG is initially employed to optimize the experimental conditions and detection of schistosomiasis japonica is conducted from human serum infected with schistosomiasis japonica reacting with the antigen of schistosomiasis attached to the nanorods.

With regard to attachment of the recognition agent goat IgG, we take advantage of functionalization of the gold nanorod surface with thiol compounds to form a self-assembled monolayer (SAM). That is, after immobilizing a layer of 11-mercaptoundecanoic acid (MUA) on the gold nanorod surface, biomolecules are covalently attached via their NH_2 groups to the COOH terminus of the MUA SAM. This is achieved by activating the carboxylic acid groups on the SAM making use of carbodiimide chemistry. As a result of the successful attachment of goat IgG on the MUA SAM, a red shift of about 19 nm in the LSPR peak is observed as shown in Fig. 1, in which the two plasmonic bands located at around 520 and 720 nm are assigned to the transversal and longitudinal modes of the electronic oscillations, respectively.

In order to form a core–shell structure on the functionalized gold nanorods, a freshly prepared $Na_2S_2O_3$ solution is mixed with the gold nanorods attached to the goat IgG. The final concentration of $Na_2S_2O_3$ is 10 mM and the reaction is conducted at 37 °C for around 2 h. The reaction progress can be monitored by the absorption spectra from 400 to 1100 nm. The longitudinal band red-shifts gradually as the reaction proceeds, and the final longitudinal wavelength of the shift depends on the reactant concentrations and reaction time. After the reaction, the nanorods are centrifuged and re-dispersed in a 10 mM Tris–HCl buffer solution for subsequent experiments. Fig. 2 depicts the TEM images. Two different phases can be clearly observed. A core of reduced gold rod and a somewhat loose shell of sulfides are disclosed by X-ray diffraction (XRD). The nanorods comprise Au crystal and complex salts consisting of Au_2S

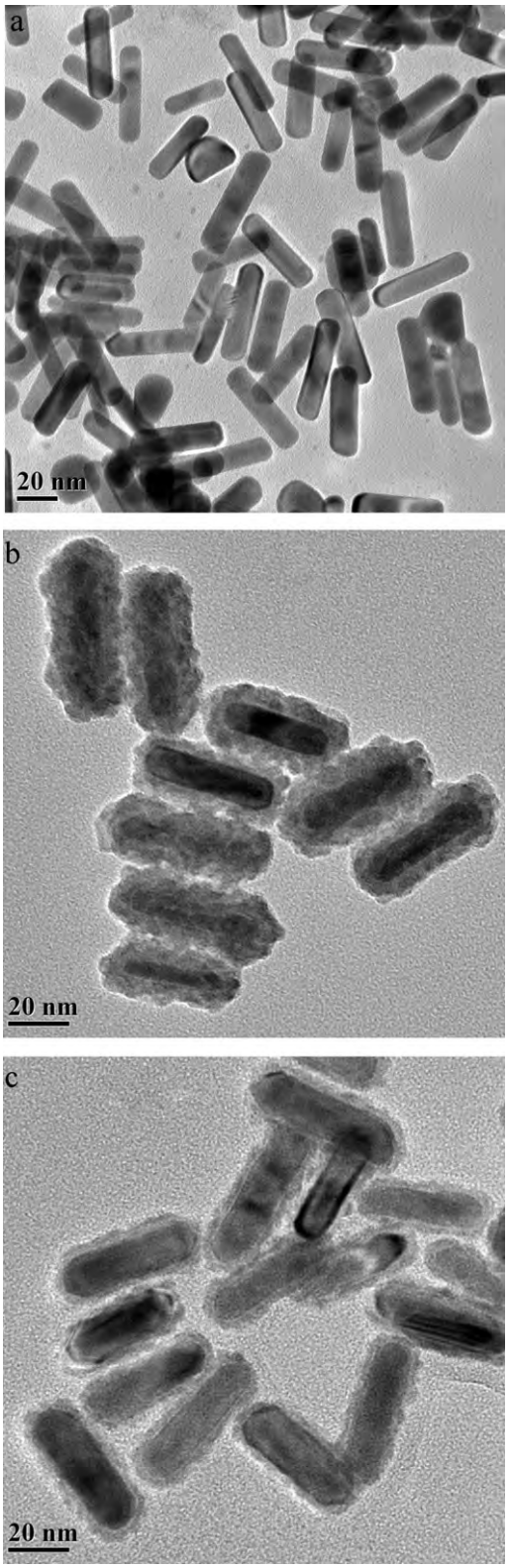

Fig. 2. TEM images of gold nanorods (a, LPW at 739 nm), the resulted composite gold nanorods (b, LPW at 891, and c, 1011 nm) at different stages.

and AuAgS. It should be noted that in addition to the expected elements of Au and S, elemental Ag is found from the nanorods which arise from the addition of $AgNO_3$ in the process to prepare the gold nanorods for better control of the shape (data not shown here and similar to previous report [35]). Interestingly, the gold nanorods prepared by seed-mediated growth can react with not only Na_2S but also $Na_2S_2O_3$ to generate the same core–shell nanocomposite. Moreover, the gold nanorods functionalized with IgG by reacting with $Na_2S_2O_3$ can also produce the similar core–shell nanocomposite. The chemical reactions between $Na_2S_2O_3$ and gold nanorods are described in the following:

$$4Au + 8S_2O_3^{2-} + 4H^+ \rightarrow 4Au(S_2O_3)_2^{3-} + 2H_2O$$

$$3Au(S_2O_3)_2^{3-} + Ag^+ + 6H_2O + 2H^+ \rightarrow Au_2S + AuAgS + 6HSO_4^- + 4H_2S$$

Accompanied by the formation of core–shell structure, a significant red-shift in the transverse and longitudinal peaks, especially the longitudinal peak, occurs. A narrow band gap semiconductor, Au_2S/AuAgS-shell, with a large refractive index at typical optical frequencies is produced in this process. The thicker the shell layer, the large is the red-shift in the longitudinal peak. It is clear that the Au_2S/AuAgS shell attached by goat IgG leads to the red-shift in the longitudinal band. In addition, as shown in Fig. 2, the generated chalcogenide shell reduces the gold nanorod along all directions. The same corrosion rate in the transverse and longitudinal directions leads to an increase in the aspect ratio of the gold nanorods further contributing to the LPW red-shift. These results demonstrate that not only gold nanorods but also gold nanorods conjugated with bio-macromolecules can form core–shell nanocomposite by reacting with $Na_2S_2O_3$. This process provides a simple and direct way to selectively adjust the LPW of functionalized gold nanorods.

3.2. Characterization of functionalized nanorods at different stages

Before the formation of the core–shell structure, gold nanorods are functionalized with goat IgG. The attachment of goat IgG to the gold nanorods relies on the Au–S chemical bond. It is necessary to investigate whether there is any change of the chemical bonding during the formation of the core–shell structure. It is critical to maintain the biomolecular activity during the process to form the core–shell structure and above all, any damage to the Au–S chemical bond should be avoided since it is the first anchoring base for the attachment of IgG onto the gold nanorods. In order to evaluate the progress, gold nanorods and functionalized gold nanorods with goat IgG are characterized by infrared (IR) spectroscopy. Fig. 3 displays the IR spectra acquired at three different functionalization stages corresponding to a layer of MUA, MUA-Au_2S/AuAgS and goat IgG-MUA-Au_2S/AuAgS, respectively. Pure gold nanoparticles do not have the characteristic stretching vibration band of organic groups, whereas most of the IR bands of MUA are observed from the MUA-modified AuNRs. In the low-frequency region, the peak at 1703 cm^{-1} arises from the acid groups of MUA conjugated gold nanorods [36]. Progressive changes in the spectra during the reaction with $Na_2S_2O_3$ to form MUA-Au_2S/AuAgS coated gold nanorods are clearly observed [37]. With the formation of a layer of Au_2S and AuAgS shell, the most obvious characteristic peaks at 1741 and 1718 cm^{-1} assigned to the ν (C=O) bands of free or non-hydrogen-bonded –COOH groups appear. With the IgG coupled to the MUA-Au_2S/AuAgS coated gold nanorods, peaks at 1643, 1153, 1144, 838, and 533 nm which are characteristic peaks of IgG similar to those previous reported [38] are observed, indicating continuous IgG attachment to the nanocomposite. Additionally, the peaks at 2851 and 2921 cm^{-1} stem from the gold nanorods functionalized with MUA, MUA-Au_2S/AuAgS coated gold nanorods, and goat IgG-MUA-Au_2S/AuAgS coated gold nanorods. Although the nanorods are washed several times, it is difficult to completely eliminate the adsorbed surfactant CTAB from the surface of the nanorods. Consequently, these two peaks can be assigned respectively to the symmetric and asymmetric C–H stretching vibrations of the acyclic alkane–CH_2– group. The peak positions are similar to those reported for pure CTAB [39]. The results demonstrate that the Au–S chemical bond resulting from the coupling between the gold nanorods and MUA is preserved on the nanorods even after the formation of the core–shell structure. This implies that the reaction is mild and highly adoptable.

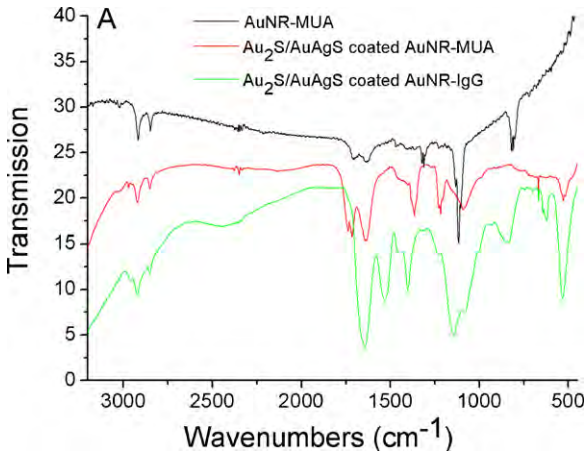

Fig. 3. FTIR spectra of MUA modified gold nanorods, MUA-Au_2S/AuAgS coated gold nanorods and goat IgG-MUA-Au_2S/AuAgS coated gold nanorods.

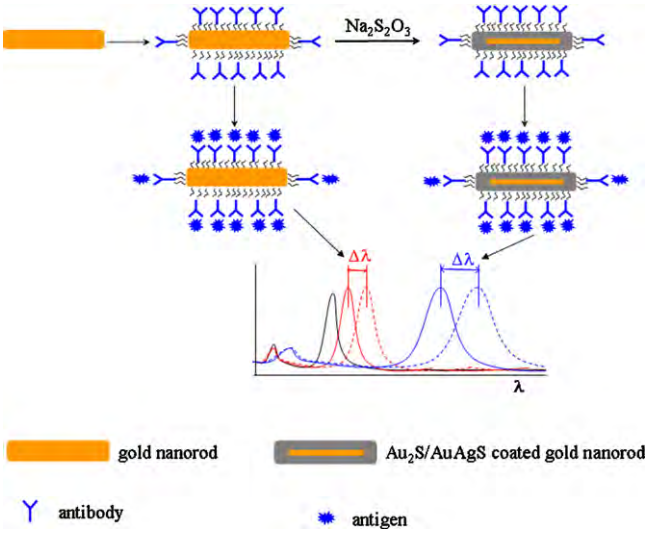

Scheme 1. Schematic illustration of a modulating plasmonic biosensor based on gradual formation of the gold nanorod composite.

As previously reported [3–7], analyte-induced aggregation of spherical gold nanoparticles results in the formation of a long wavelength band and a broader plasmon peak. Similarly, the end-to-end assembly of gold nanorods can induce a significant red-shift in the LPW as well as broader plasmon peak. According to Fig. 2 and the above discussion, LPW red-shift results from the formation of the core–shell structure and changes in the aspect ratio of the reduced gold nanorods core, but not induced by aggregation of the nanorods. The mechanism is illustrated in Scheme 1. The significant red-shift after forming the shell on the gold nanorods is shown together with the increased wavelength response compared to the ones with the shell.

3.3. Comparison of sensitivity of biosensor with different LPW

The reaction changes the aspect ratio of the gold nanorods as illustrated in Fig. 2. In theory, a small variation in the aspect ratio can lead to a drastic change in the plasmon spectra. To investigate the effects of the $Na_2S_2O_3$-reaction-induced red-shift on the sensing sensitivity, two types of gold nanorods, bare gold nanorods (LPW at 739 nm) and Au_2S/AuAgS-coated gold nanorods (LPWs at 891 and 1011 nm) are studied. The amounts of the different nanorods attached by goat IgG and added rabbit anti-goat IgG are equal (the rabbit anti-goat IgG concentration is 2×10^{-10} M).

When multiple washing steps are incorporated to remove unbound analytes or the samples are added to the modified nanorods during the experimental process, uncertain changes in the nanoparticle concentration may occur and alter the absorption intensity, thus rendering the monitoring of biospecific interaction events inaccurate. However, the changes in LPW are directly responsible for the changes in the refractive index in the vicinity of the nanorods [1], and so they form the basis of quantitative analysis utilizing the specific reaction between antibody and antigen. Fig. 4 shows a significant red-shift after the reaction with relative standard deviations (RSD) of 3.3–5.4% ($n = 3$). The degree of red-shift depends on the type of ligand-receptor binding. The Au_2S/AuAgS-coated gold nanorods with LPWs at 891 and 1011 nm exhibit large red-shifts of 28 and 40 nm, respectively, whereas only a 12 nm shift is observed from the bare ones. Hence, more coated nanorods provide more sensitive monitoring of the affinity events. The wavelength dependence of the longitudinal plasmon peaks on the nanorods and corresponding changes in the refractive indices in the immediate vicinity make Au_2S/AuAgS-coated gold nanorods extremely sensitive to molecular binding events.

3.4. Detection of schistosomiasis japonica

An important consideration is the biomolecular activity during the formation of the core–shell structure. The gold nanorods functionalized with biomolecules should not be destroyed because they are essential in the design of a tunable wavelength biosensor for further applications. Therefore, a practical application in detecting schistosomiasis japonica is carried out to evaluate this biosensor. The antigen of schistosomiasis japonica is attached to the gold nanorods and a red-shift appears as shown in Fig. 5. A clear red-shift of 12 nm occurs after the antigen of schistosomiasis japonica attaches to the gold nanorods. After the reaction between $Na_2S_2O_3$ and the functionalized gold nanorods at 37 °C for 40 min, a clear

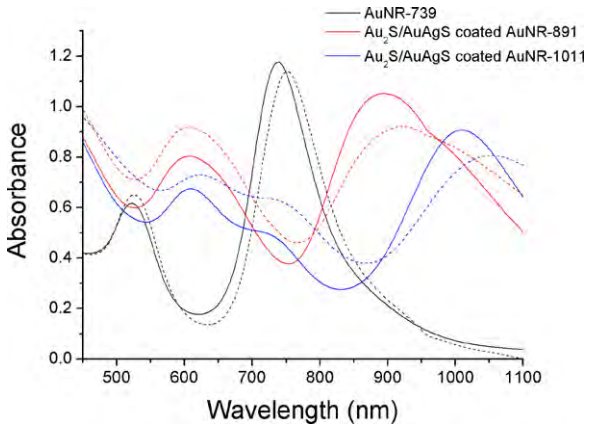

Fig. 4. Three pairs of absorption spectra corresponding to the three types of nanorods as shown in Fig. 2. Each pair shows that the red shift resulted from the recognition of rabbit anti-goat IgG with goat IgG attached on the different types of nanorods.

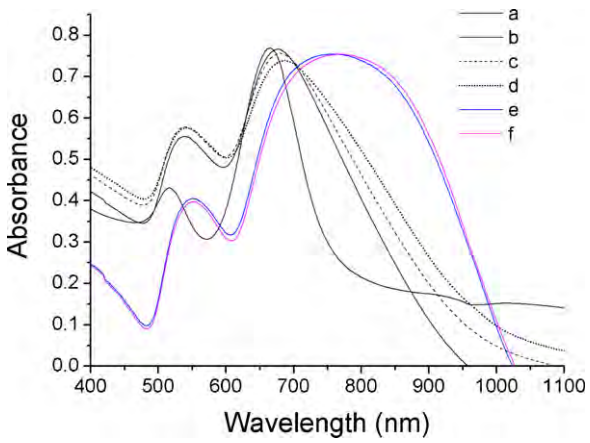

Fig. 5. Absorption spectra of antigen of schistosomiasis japonica conjugated gold nanorods and the resulting Au_2S/AuAgS coated gold nanorods attached by schistosomiasis japonica react with human serum infected with schistosomiasis japonica, respectively. (a) represent the as-synthesized gold nanorods, (b) is antigen of schistosomiasis japonica conjugated gold nanorods, and different human serum concentration infected with schistosomiasis japonica (c) (1:3600) and (d) (1:5000) react with antigen of schistosomiasis japonica conjugated gold nanorods, (e) represents Au_2S/AuAgS coated gold nanorods attached by schistosomiasis japonica obtained by a, (f) represents human serum (1:10000) infected with schistosomiasis japonica react with antigen of schistosomiasis japonica conjugated Au_2S/AuAgS coated gold nanorods.

LPW red-shift from 678 to 761 nm is observed. We have checked the detection ability of the immobilized antigen by conducting experiments using a mixture of antigen of schistosomiasis japonica conjugating nanorods and human serum infected with schistosomiasis japonica. When the human serum with schistosomiasis japonica is diluted 1:50,000 (volume ratio, serum/Tris–HCl buffer), the LPW may be detectable. When it is increased to 1:10,000, a 12 ± 1 nm ($n = 3$) red-shift is clearly observed as shown in Fig. 5f. Hence, the antibodies to the antigen of schistomiasis are generated in the serum infected by schistomiasis japonica and the antibodies specifically react with the antigen of schistomiasis leading to the LPW red-shift. In the control experiments involving normal human serum without infected schistosomiasis japonica, there is no change in the LPW. A comparison is also performed between the serum infected with schistosomiasis japonica and another aliquot of original gold nananorods (unshelled gold nanorods) attached by the antigen of schistosomiasis. There is no significant change in the LPW until the concentration of human serum infected with schistosomiasis japonica is larger than 1:5000 (Fig. 5c). When the ratio goes up to 1:3600 (Fig. 5d), a 8 nm red-shift in LPW is found. At the same time, the same concentration of normal human serum without infected schistosomiasis japonica does not produce any detectable signal. Although 6 of these 10 healthy samples show slight response with the change in the LPW being less than 2 nm compared to an average red-shift of 0.8 nm, 4 specimens indicate no red shift in the LPW at all (0 nm). These results indicate good biological activity of the attached antigen of schistosomiasis after the reaction and the nanocomposite offers higher sensitivity than the bare gold nanorods.

4. Conclusion

We demonstrate a novel method to adjust the sensitivity of LSPR sensors suitable for the specific detection of biomolecules via immunological recognition. The innovation in this new approach is that the localized surface plasmon resonance property may be adjusted after attachment of the recognition reagent. This leads to a lager red-shift in the longitudinal LSPR absorption compared to the bare gold nanorod sensors and thus offers greatly

enhanced sensitivity in the detection of schistosomiasis japonica. It is selectively tailoring plasmonic resonant wavelength LSPR sensors based on functionalized nanorods for highly sensitive detection of biomolecules. This technique can be easily extended to the preparation of other sensors based not only on immunorecognition but also on other types of specific reactions.

Acknowledgments

This work was supported by Hunan Provincial Natural Science Foundation of China (10JJ5004), Natural Science Foundation of China (Nos. 90717120, 21075035), Hong Kong Research Grants Council (RGC) General Research Funds (GRF) No. CityU 112307, and City University of Hong Kong Strategic Research Grant (SRG) 70080009.

References

[1] J. Pérez-Juste, I. Pastoriza-Santos, L.M. Liz-Marźan, P. Mulvaney, Coordin. Chem. Rev. 249 (2005) 1870–1901.
[2] M.C. Daniel, D. Astruc, Chem. Rev. 104 (2004) 293–346.
[3] C. Xie, F. Xu, X. Huang, C. Dong, J. Ren, J. Am. Chem. Soc. 131 (2009) 12763–12770.
[4] S.K. Lee, M.M. Maye, Y.B. Zhang, O. Gang, D. Lelie, Langmuir 25 (2009) 657–660.
[5] Y. Zu, Z. Gao, Anal. Chem. 81 (2009) 8523–8528.
[6] X. Xu, N.L. Rosi, Y. Wang, F. Huo, C.A. Mirkin, J. Am. Chem. Soc. 128 (2006) 9286–9287.
[7] K. Cho, Y.C.H. Lee, K. Lee, Y. Kim, H. Choi, P.D. Ryu, S.Y. Lee, S.W.J. Joo, Phys. Chem. C 112 (2008) 8629–8633.
[8] Z. Ma, L. Tian, T. Wang, C. Wang, Anal. Chim. Acta 673 (2010) 179–184.
[9] K.L. Kelly, E. Coronado, L.L. Zhao, G.C. Schatz, J. Phys. Chem. B 107 (2003) 668–677.
[10] A.J. Hallock, P.L. Redmond, L.E. Brus, Proc. Natl. Acad. Sci. 102 (2005) 1280–1284.
[11] J.S. Lee, P.A. Ulmann, M.S. Han, C.A. Mirkin, Nano Lett. 8 (2008) 529–533.
[12] L. Li, B. Li, Analyst 134 (2009) 1361–1365.
[13] K.K. Caswell, J.N. Wilson, U.H.F. Bunz, C.J. Murphy, J. Am. Chem. Soc. 125 (2003) 13914–13915.
[14] Z. Sun, W. Ni, Z. Yang, X. Kou, L. Li, J. Wang, Small 4 (2008) 1287–1292.
[15] A. Figuerola, I.R. Franchini, A. Fiore, R. Mastria, A. Falqui, G. Bertoni, S. Bals, G.V. Tendeloo, S. Kudera, R. Cingolani, L. Manna, Adv. Mater. 21 (2009) 550–554.
[16] M. Sethi, G. Joung, M.R. Knecht, Langmuir 25 (2009) 1572–1581.
[17] A.S. Barnard, L.A.J. Curtiss, Mater. Chem. 17 (2007) 3315–3323.
[18] C. Yu, J. Irudayaraj, Anal. Chem. 79 (2007) 572–579.
[19] W.S. Kuo, C.N. Chang, Y.T. Chang, C.S. Yeh, Chem. Commun. (2009) 4853–4855.
[20] L. Tong, Y. Zhao, T.B. Huff, M.N. Hansen, A. Wei, J.X. Cheng, Adv. Mater. 19 (2007) 3136–3141.
[21] M.M. Mille, M. Lazaride, Y. Cui, L. Manna, J. Li, L.W. Wang, Nature 430 (2004) 190–195.
[22] T. Molari, E. Rothenberg, I. Popov, R. Costi, U. Banin, Science 304 (2004) 1787–1790.
[23] C. Wu, Q.H. Xu, Langmuir 25 (2009) 9441–9446.
[24] T. Kawano, Y. Niidome, T. Mori, Y. Katayama, T. Niidome, Bioconjugate Chem. 20 (2009) 209–212.
[25] D.K. Yi, S.T. Selvan, S.S. Lee, J. Am. Chem. Soc. 127 (2005) 4990–4991.
[26] W.E. Doering, M.E. Piotti, M.J. Natan, Adv. Mater. 19 (2007) 3100–3108.
[27] C.H. Liang, C.C. Wang, Y.C. Lin, C.H. Chen, C.H. Wong, C.Y. Wu, Anal. Chem. 81 (2009) 7750–7756.
[28] J.D. Qiu, H.P. Peng, R.P. Liang, X.H. Xia, Biosens. Bioelectron. 25 (2010) 1447–1453.
[29] N. Berhe, G. Medhin, B. Erko, T. Smith, S. Gedamu, D. Bereded, R. Moore, E. Habte, A. Redda, T. Gebre-Michael, S.G. Gundersen, Acta Trop. 92 (2004) 205–212.
[30] B. Gryseels, K. Polman, J. Clerinx, L. Kestens, Lancet 368 (2006) 1106–1118.
[31] Y.B. Zhou, M.X. Yang, P. Tao, Q.L. Jiang, G.M. Zhao, J.G. Wei, Q.W. Jiang, Acta Trop. 107 (2008) 251–254.
[32] J.M. Yu, S.J. de Vlas, Q.W. Jiang, B. Gryseels, Parasitol. Int. 56 (2007) 45–49.
[33] A. Brioude, X.C. Jiang, M.P. Pileni, J. Phys. Chem. B 109 (2005) 13138–13142.
[34] L. Gou, C.J. Murphy, Chem. Mater. 17 (2005) 3668–3672.
[35] H. Huang, X. Liu, Y. Zeng, X. Yu, B. Liao, P. Yi, P.K. Chu, Biomaterials 30 (2009) 5622–5630.
[36] R.V. Duevel, R.M. Corn, Anal. Chem. 64 (1992) 337–342.
[37] L. Ren, G.M. Chow, Mater. Sci. Eng. C 23 (2003) 113–116.
[38] C. Petibois, G. Cazorla, A. Cassaigne, G. Déléris, Clin. Chem. 47 (2001) 730–738.
[39] C.L. Kuo, M.H. Huang, J. Phys. Chem. C 112 (2008) 11661–11666.